Published in final edited form as:
Biochim Biophys Acta. 2007 May ; 1768(5): 1238–1246.

Structural and Functional Recovery of Electropermeabilized Skeletal Muscle *in-vivo* after Treatment with Surfactant Poloxamer 188

John M. Collins, **Florin Despa**, and **Raphael C. Lee**
Electrical Trauma Research Program, Departments of Surgery, Medicine and Organismal Biology and Anatomy, The University of Chicago, Chicago, Illinois 60637

Abstract

A critical requirement for cell survival after trauma is sealing of breaks in the cell membrane [1–11]. The triblock copolymer surfactant Poloxamer 188 (P188) is known to increase the cell survival after membrane electroporation [8,22]. Here, we use a rat hind-limb model of electroporation injury to determine if the intravenous administration of P188 improves the recovery of the muscle function. Rat hind-limbs received a sequence of either 0, 3, 6, 9, or 12 electrical current pulses (2 ampere, 4ms duration, 10s duty cycle). Magnetic resonance imaging (MRI) analysis, muscle water content and compound muscle action potential (CMAP) amplitudes were compared. Electroporation injury manifested edema formation and depression of the CMAP amplitudes. P188 (one bolus of 1mg/ml of blood) was administrated 30 or 60 minutes after injury. Animals receiving P188 exhibited reduced tissue edema ($p < 0.05$) and increased CMAP amplitudes ($p < 0.03$). By comparison, treatment with 10kDa neutral dextran, which produces similar serum osmotic effects as P188, had no effect on post-electroporation recovery. Noteworthy, the present results suggest that a single intravenous dose of P188 is effective to restore the structural integrity of damaged tissues with intact circulation.

Keywords

Electroporation; Poloxamer 188; skeletal muscle; Action potential; MRI

INTRODUCTION

Loss of structural integrity of the cell membranes is a central path leading to tissue necrosis following all forms of trauma. Electrical current causes tissue injury by both electroporation [1,2] and heating [3,4]. Loss of membrane integrity and function due to structural breakdown is a basic element in the pathogenesis of cell injury by either electroporation or heat injury [4,5]. Therefore, the development of therapeutic strategies to restore the structural integrity of damaged cells would have potentially important applications to electrical injury victims.

Electroporation is associated with the formation of transient or stable structural defects, or “pores”, in cell membranes [1,2]. Formation of large stable transient defects that do not spontaneously seal inexorably results in metabolic cellular energy depletion as membrane ion

Corresponding author Raphael C. Lee, MD, ScD, Department of Surgery, The University of Chicago, 5841 S. Maryland Avenue, Chicago, Illinois 60637, Phone: (773)702-6302, Fax: (773)702-1634 r-lee@uchicago.edu

pumps increase their activity in an attempt to maintain transmembrane ionic balance. This situation results in acute cellular necrosis. Thus, an important consideration in discussing electrical shock mediated tissue injuries, is the dynamics of cell membrane electroporation [2,6]. Small defects, which do not exceed the size of a few water molecule diameters, reseal spontaneously [7], while larger defects will reseal only after alteration of molecular interactions [8].

Poloxamer 188 (P188), which is a biocompatible polymer consisting of two hydrophilic side-chains attached to a hydrophobic center core, has been shown capable of sealing stable defects cell membranes after various types of trauma [8–11]. Furthermore, experiments using monolayer lipids indicate that P188 molecules insert into holes, induce reordering of membrane lipids that results in sealing of defects, and then are squeezed out [12,13].

Various reports [8–10,12–14] have described the essential conditions for P188 mediated membrane sealing in various types of cells. It has been established that the surfactant monomer is the active agent, not the surfactant micelle. For membrane sealing purposes, P188 is typically administrated at concentrations well below the critical micelle concentration (CMC) of 0.1–1.0 mM (about 1–10 mg/ml) at physiological temperatures. Although it is well established that P188 can increase survival of electroporated muscle cells [8], it has not been shown yet that P188 sealed muscle will recover function. Our focus here is to rigorously monitor, *in vivo*, the effects of P188 administration in an electrically injured animal model and demonstrate that P188 improves the functional recovery of the damaged muscles.

To quantify the functional recovery of injured muscles following membrane sealing we employed compound muscle action potential (CMAP) measurements using skin surface electrodes and magnetic resonance imaging, which are both non-invasive methods. The ability to generate an action potential depends on cells ability to establish a transmembrane potential required to properly configure voltage gated ion channels [15]. This requires ATP generation to fuel the various ion pumps in the cell membrane. Loss of membrane integrity results in the inability to produce an action potential. Thus, the CMAP amplitude should reflect muscle membrane integrity. Proton weighted magnetic resonance imaging (MRI) can provide information about the state of hydration of the cellular components [16]. If skeletal muscle membranes are disrupted, an osmotic swelling of the cells follows. This leads to changes in the magnetic resonance (MR) relaxation kinetics. Restoration of the intracellular water content requires restoration of the membrane integrity and normal ionic balance. Thus, MRI is an effective way to monitor the recovery of the structural integrity and function of the plasma membrane.

The goal of this study is twofold. First, we investigate whether sub-CMC levels of P188 results in restoration of ionic concentration balance across the cell membrane as measured by MRI and, second, we examine if the structural restoration of the muscle also improves its ability to generate action potentials stimulated by motor nerve activation.

METHODS

Anesthesia protocol

Anesthesia was induced in Female Sprague-Dawley rats (300 ± 20 g, each) by 5% isofluorane. An intraperitoneal (IP) injection of ketamine (28 mg/ml) and xylazine (0.20 mg/ml), at a dose of 0.35 ml/hr was given throughout to maintain the anesthesia at the surgical plane. Supplemental oxygen was administered throughout the procedure. Heart rate, blood oxygen saturation (Sa02%), respiration, and temperature were monitored throughout the experiment. The animal was sacrificed at the end with an overdose (20mg/kg) of Xylazine. The following

protocol was approved by the University of Chicago Institutional Animal Care and Use Committee.

Hind-limb Muscle Electroporation

The rats were electro-shocked by a discharge-type rectangular pulse generator (Dialog, Dusseldorf, Germany). Electrical pulses of 2kV, 2A, 4ms duration, separated by a 10s interval to allow for thermal relaxation [6], were delivered along an electrical conduction path encompassing the entire length of the left leg, between the ankle and the base of the tail (Fig. 1). The skin along this pathway was abraded circumferentially and wrapped in gauze soaked in Parker Electrode Gel. Stainless-steel cuff electrodes were attached to gauze soaked gel salt bridges and connected via high voltage cables to the pulsed current source. The impedance of this circuit at 100 Hz was in the range of 700 to 1000 Ω. Rats received 3, 6, 9, and 12 electrical shocks that progressively increased the level of injury in muscles along the electric current pathway.

Histology

Shock exposed and non-exposed muscles were harvested for histological analysis (see Fig. 2). Biopsies were taken 6 hours after electrical shocks from controls and injured legs of rats monitored by surface electromyography (EMG). The entire biceps femoris muscle was surgically removed and samples (both longitudinal and transverse, 7 micron thick, sections) were extracted from the mid-belly region of the muscle. Tissues were fixed in 10% formalin, the samples were then paraffin embedded, cut, slide mounted and Hematoxylin and Eosin stained (H&E). The histological analysis revealed that the pattern of injury in the muscle varies from one area to another.

Pharmaceutical therapy

All animals received an intravenous lactated ringers (LR) bolus immediately after injury, or sham injury, as fluid resuscitation. The amount of LR was adjusted adequately to maintain adequate urine output throughout the experiment. In the present study, the treatment was given at different times, depending on which outcome variable was being measured. Thus, animals monitored by surface electromyography received P188, Dextran or LR, 30 minutes post-electroporation, which coincides with the time at which minimal recovery of the muscle activity was detected by EMG. For the MRI studies, the treatment was administered when edema started to develop, 60 minutes post-shock, approximately. In this way, we were able to evaluate precisely the improvement in recovery following the pharmaceutical intervention.

All animals received intravenously an additional 1ml bolus of LR fluid to maintain intravascular volume. Control-treated rats received 1ml of LR fluid without P188. P188-treated rats received 1 ml LR+P188 (3.0 mM Pluronic F68, Medical Grade; Anatrace, Inc., Maumee, OH), and dextran-treated rats received 1ml LR + dextran (3.0 mM, MW=10 kDa, BASF, Mount Olive, NJ). Based on extracellular fluid volume, which was estimated as 24% total body weight [17], P188-treated rats received a dose such that the final concentration of P188 in the blood was 0.15mM, which is below CMC [12].

Magnetic Resonance Imaging

Cell membrane disruption leads to an osmotic swelling of the injured cell. Cell injury also leads to inflammatory cytokine production which causes interstitial swelling of the injured tissue as well. The state of water in the injured area is changed and the compartmentalization and dynamics of the water proton populations during magnetic relaxation differ from a healthy tissue. Spin-spin relaxation time (T_2)-MRI, which is very sensitive to the change in tissue hydration, is, therefore, a useful tool to characterize the injury. By looking at the histological

samples displayed in Fig. 2, we can observe regions of vacuolization in the injured muscles, which suggests increased water within damaged myocytes. Indeed, the rats subjected to 12 electrical shocks have marked "contraction-band necrosis" to most cells and severe edema. This level of injury seems suitable for monitoring the edema formation by MRI.

***In-vivo* MRI Studies—**For the *in vivo* T_2 -MRI experiment, we used a custom made Helmholtz pair coil with internal diameter of 25mm. T_2 - weighted images were acquired with a standard multiple echo spin-echo Carr-Purcell-Meiboom-Gill (CPMG) sequence with the following parameters: Repetition time (TR) = 1s; equally spaced echo times (TE) between 10 and 100ms. The image matrix was 128x128 pixels on a field of view 50mm. Each spin-echo image acquisitions lasted 3.33 minutes.

First, we performed a preliminary MRI assessment of the injury to monitor the development in time of the edema. T_2 was measured on several 5 x 5 pixel regions selected on the injured leg (n=5). The values were averaged over these regions and followed from 60 minutes post-shock to 180 minutes post-shock, when T_2 reached a saturation plateau and edema fully developed (see Fig. 3). The behavior of the T_2 values through the time period of 1–3 hours was studied for healthy and injured tissue.

Details about the extent of the injury and evolution after treatment can be obtained by constructing histograms of the intensity of the magnetic relaxation of water in the injured tissues. Ten axial slices were prescribed 2mm thick and separated by 2mm over the entire mid-thigh region of the leg. Imaging began at approximately 1h after shock and multiple echo spin-echo scans were performed every 5 minutes until 3h post-shock. For each image acquisition, the MRI signal intensities at imposed TE measured in each voxel were fitted to an exponential decay. Thus, T_2 values corresponding to each particular voxel were derived. We then evaluated the number of pixels per slice at each T_2 value in the domain 30–100 ms using the ImageJ (NIH) program [19]. The total number of pixels per leg at each T_2 value was determined by summing over all ten slices. Then, the mean number of pixels at each T_2 value in the interval 30–100 ms was determined for non-injured, control (injured) LR treated rats (n=5) and P188 treated rats (n=5) at the initial and final time points.

***Ex-vivo* MRI Studies—**Proton magnetic resonance images were recorded using a Bruker scanner (Bruker Biospin, Billerica, MA, USA) (200 MHz) equipped with a 4.7 T, 28-cm internal diameter superconducting magnet and actively shielded magnetic field gradients.

After edema fully developed (three hours post-shock), the rat was sacrificed and the *soleus* (SOL), *extensor digitorum longus* (EDL), and *biceps femoris* muscles (BFM) were harvested from both shocked and control legs. The muscles were then placed in 1x1x5cm cuvets, sealed, to prevent water evaporation, and put into a MRI coil. T_2 - weighted images were acquired with a standard multiple echo spin-echo CPMG sequence with the following parameters: TR=2s; equally spaced TE between 10 and 100ms and slice thickness (ST) = 2 mm. The image matrix was 128x128 pixels on a field of view 50mm. We also recorded several spin-lattice relaxation time (T_1)- weighted images with a resolution of 256x256 pixels, for which the recording parameters were set at TR = 400 ms and TE = 5 ms, respectively.

Five sets of samples from five different rats were used. In each set, one leg was shocked and the contralateral leg from the same rat was used as a control. T_2 values were measured by a standard procedure in which the values of the signal amplitude from the echoes of the multi-echo, spin-echo experiments are fitted to the spin-spin signal decay equation [18]. Following MRI measurements the tendons were removed from the explants and muscle wet weight was determined. Then, the muscles were placed in a vacuum oven at 60°C for 36h, until completely dry, in order to obtain the dry weight of the muscle. The value of the water content of the muscle

tissue was derived. We checked for any possible error on the hydration data due to a possible evaporation during MRI measurements. Thus, a similar electroporation protocol was conducted on three additional rats, which were then sacrificed at 3 hours post-shock, after edema fully developed. The muscles were harvested, wet weights were determined, and then the muscles were allowed to dry. The measurements showed that these extra hydration data were in the same margins as above (data not shown) and, therefore, no evaporation occurred during MRI experiments. Other details of the *ex vivo* protocol and image acquisitions are published elsewhere [18].

Surface electromyography

A clear indication of muscle and nerve cell function is the ability to generate and conduct action potentials. Repetitive conduction of action potentials requires an intact membrane and cellular ATP production. The electroporation of nerve and muscle membranes has been shown to reduce the action potential of peripheral nerves [20]. Thus, measurement of the magnitude of CMAP amplitudes provides meaningful information regarding the functional status and viability of skeletal muscle tissue. Surface electromyography permits non-invasive recording of CMAP using skin electrodes [21].

We recorded CMAPs by using commercially available electromagnetic coils (Dantec® Neurodiagnostic Equipment). In our setup, a magnetic pulse provided by a coil placed above the spinal cord in the lower back of the anesthetized rat stimulates the nerves in a way similar to conventional electrical stimulation [21]. Synchronized with the electromyographic recorder (Dantec® Counterpoint), the MagLite® Stimulator sends a magnetic field pulse through the probe. CMAPs are recorded using platinum surface electrodes placed over the *biceps femoris* at ½ hour intervals for a period of 6h. At 5h, the sciatic nerve is blocked with lidocaine to verify that CMAP is nerve stimulated. Control CMAPs are recorded from the opposite thigh, which was not shocked.

RESULTS

Animal responses

All animals were well anesthetized for the experiments and all survived until terminated. Anesthesia depth was assured by the absence of papillary reflexes or responses to toe pinch. There were no burning or other visible signs of thermal injury. The electroporation protocol used in this work is similar to that proposed by Block *et* al. [6] in which peak measured muscle temperature rise in the hindlimb muscles was less than 1 °C. There was no burning at the skin contacts, either because the epidermis was removed and/or the contact points were soaked with 4 mL KCl solution.

Following electroporation injury, all the animals exhibited physiological signs of trauma immediately following injury such as decreased heart rate, urine output and SaO_2. However, these parameters were recovered at normal physiological values within 15 to 30 minutes after injury using the fluid resuscitation protocol described above.

Consequences of skeletal muscle electroporation

In Fig. 2 we display representative phase contrast photomicrographs (40x) of H&E stained 7 *μm* sections of electrically shocked biceps femoris muscles. Biopsies were taken from controls and injured legs of rats that were monitored by surface EMG. Electroporation damage is distributed very non-uniformly in each muscle reflecting the stochastic nature of electroporation. The more shocks the more severe and the more uniform the damage. Longitudinal sections from muscle exposed to (a) 3 shock pulses exhibit a low percentage of damaged cells with mostly normal cytoskeletal architecture and some interstitial edema.

Muscles subjected to 6 shocks (b) manifest damage to 20–30% of the cells with more edema. Muscle subjected to 9 and 12 shocks (c) display marked "contraction-band necrosis" to most cells and severe edema. Over the six hour period following electroporation injury, the depression in CMAP amplitudes was very transient for muscles exposed to 3 and 6 shocks, respectively. Also, test experiments indicated that the administration of P188 in these groups made no significant difference, although there was a trend toward faster recovery in the 6 shock group. Consequently, rats subjected to 3 and 6 shocks were deemed irrelevant for the purpose of the present study and we did not investigate them further. Characteristic CMAP data of control and injured legs for 9 and 12 shock groups are displayed in Fig. 4. We noticed a profound depression in the CMAP amplitudes that persisted in the LR and Dextran treated groups throughout the 6 hours post-shock. In rats which received 12 electrical pulses, these data show a severe inability of injured muscles to generate an action potential. We observed that the spontaneous recovery of the CMAP amplitude is higher in rats which received only 9 electrical pulses. Based on these data and on the histological analysis (Fig. 2), we decided to perform the functional recovery assay on rats which received 9 electrical pulses. The level of injury inflicted in these rats can facilitate a proper observation of any improvement in recovery following the pharmaceutical intervention. In addition, we can observe that the increase of the CMAP amplitudes is sufficiently slow in this six hour period. On this time scale, we can efficiently monitor the result of the pharmaceutical intervention and detect any possible harmful effect. The slight decline of the CMAP amplitudes in controls, which can be noticed in Figs. 4 and 7, is a typical manifestation of the anesthesia.

By looking at Fig. 3, we can see that the i*n vivo* T_2 values for the injured leg (12 shocks) increase significantly in time, which is a sign of edema formation. Direct observation also revealed swelling of the injured region. The edema seems to be fully developed after 3 hrs post-shock, when T_2 achieved the saturation plateau. Characteristic *ex vivo* T_2 values for control and injured SOL, EDL, and BFM samples surgically extracted at 3 hrs post-shock, and their water content, are displayed in Fig. 5. T_2 values in various damaged muscles are 20 – 108 % larger (Fig. 5a), and so is the hydration level, 4 – 15 % higher (Fig. 5b). Edema raises the local hydration level over its physiological value, which leads to an increase of T_2 .

Evaluation of the pharmaceutical intervention

We found that the intravenous administration of P188 leads to a significant reduction of edema. The result of P188-treated rats is compared to that corresponding to LR-treated (which serve as control for injury) and dextran-treated rats. From Fig. 5 we can observe a significant difference between T_2 values corresponding to the three muscle types extracted from healthy rats and those extracted from LR-treated and dextran-treated rats, respectively. The difference is significantly reduced when compare to the P188-treated rats. One can also notice that, practically, LR and dextran treatments lead to a similar outcome of the recovery, which means that dextran is not a sealing agent for disrupted membranes. It is interesting to note that T_2 values for EDL and BFM in P188-treated rats are similar to those corresponding to the non-shocked legs. A significant increase in hydration after injury can be noticed in both treated and non-treated rats. However, the increase of the water content in P188-treated rats was smaller than in the rest. The evolution of the hydration level in dextran-treated rats showed a similar behavior with that corresponding to LR-treated rats. A similar trend can be noticed for EDL but not for BFM, where P188 treatment practically showed no effect on the hydration level.

Based on the lack of influence of dextran in the recovery process of the electrically injured muscles we, therefore, continued with *in-vivo* studies only for P188-treated rats. Figure 6 displays the average number of pixels for each T_2 value in the interval 30–100 ms for healthy (a) LR-treated (b) and P188-treated (c) rats. The amplitudes and distribution of the T_2 values reveal a rather complex relaxation decay of the magnetic signal. For instance, one can see that

the T_2 value distribution in the domain $30ms \leq T_2 \leq 40ms$ is clearly distinct from that corresponding to $T_2 > 40ms$, which may indicate that this electroporation injury model of edema display two components of the magnetic relaxation of water, as recently reported for a rat muscle edema model [22]. However, we can also notice that the amplitudes of T_2 are significantly higher on the entire domain, between 30ms and 100ms. These data are most consistent with a multiexponential relaxation behavior of tissue water [23–26]. Generally, the number of magnetically distinguishable water environments corresponding to the magnetic relaxation behavior presented in Fig. 6 (a, b and c) can be estimated by fitting the intensity of the signal to a multiexponential equation [24,26]. Interpretation of the MR data in terms of a multiexponential relaxation decay or, alternatively, by showing histograms of the intensities of the magnetic signals, as those displayed in Fig. 6, can provide useful information about the overall physiological changes of water in injured tissue.

We can observe that the injury leads to modifications of the *in vivo* T_2 values on a large scale (from 30ms to about 80ms, and over). Generally, we can see a pronounced shift of T_2 towards larger values, which is consistent with the result of the *ex vivo* MRI measurements. Thus, the average pixel numbers corresponding to T_2 values larger than 40ms increase at the expense of those below 40ms, which decrease in time for injured control (LR-treated) rats. To better reveal the effect of treatment, we can use a pictorial representation of the evolution of the volume of injury as displayed in Fig. 6d. Thus, by subtracting at each T_2 value the average pixel number characterizing healthy rats from that corresponding to injured (LR- and P188-treated, respectively) rats, we can observe the evolution of the injury at various times of the therapeutic intervention. Here, we can observe that, in average, the reduction of the injury volume in P188 treated rats at the end point (3h post injury), as derived from the pixel number distribution, is about 23%.

In Fig. 7 we present relevant results showing that the treatment of shocked rats with P188 increased the CMAP amplitudes of the injured muscles towards the level measured before the injury. Easy algebra shows that the area under the CMAP amplitude curve of P188-treated rats is, on average, about 41% larger than that corresponding to injured, non-treated rats (see Fig. 4). Fig. 8 shows that the magnetic signals of water in muscle treated by P188 and non-injured muscles are fairly similar. This suggests that the water balance across plasma membrane was reestablished, which means that the membrane integrity and function was recovered after the treatment with P188.

DISCUSSION

The recent paper by Matthews [27] and the results presented here demonstrate that surfactant sealed cells are more capable of regaining functionality then untreated cells. We demonstrated by using MRI techniques that the intravenous administration of a P188 bolus leads to a structural restoration of the compromised cell membranes in the injured muscles. Untreated controls do not improve indicating the defects in the electroporated membranes remain stable. The evolution of the transverse magnetic relaxation time (T_2) of water protons in electroporated muscles along with measurements of the water content in those muscles reveal that P188 arrests the edema which could only occur if the cell membranes were sealed. We can observe (see Figs. 6d and 8) the shift back of the magnetic response of water towards values corresponding to normal protein hydration. Second, we present data obtained by a non-invasive surface electromyography technique that show that P188 administration enhances the functional recovery of the injured muscles. Thus, treatment with P188 reinstalled the ability of damaged muscle and nerve cells to generate and conduct action potentials.

One can conclude that a combined MRI-EMG approach is capable of assessing the extent of muscle injury, as well as monitoring structural and functional recovery after pharmaceutical

intervention. Because of the large magnitudes of pixel intensities in the T_2 distribution displayed in Fig. 6, it is reasonable to suggest that electroporation injury has a profound effect on the multicomponent T_2 relaxation of muscle. Though the MRI analysis presented here proves very informative for detecting physiological changes in injured tissues, it becomes less specific in describing the pathological aspects of these changes. Increasing signal intensity on T_2 -weighted MR images of muscle can reflect a range of pathologies, including various types of edema, necrosis, inflammation, and fatty infiltrations [28]. Hence, the MRI method used in the present study is rather nonspecific and does not give insight into the cell damage mechanism. However, improved insights could be obtained in the same experimental setup by using other MRI methods. Further studies are required to decipher the number of distinct T_2 components characterizing the magnetic relaxation of water in electroporated muscles, as well as the temporal evolution of these components during muscle recovery.

Both *ex vivo* and *in vivo* measurements revealed structural and functional recovery of the injured muscles after intravenous administration of P188. Several other reports emerged in literature presenting therapeutic strategies to accelerate the cell membrane repair after various injuries [29–31]. Thus, the evidence is mounting that P188, or similar triblock copolymers, may be a potential treatment for humans who have experienced an electrical injury. The comparison between the results of P188 and dextran treatments shows that the latter has no effect on muscle recovery, which suggests that the arrest of edema in P188-treated rats is not due to osmotic effects and that P188 effectively seals injured membranes. In future work, other surfactants with varying ratios of hydrophilic to hydrophobic domains will be tested using this protocol of electroporation injury, in order to identify the characteristics of a compound which will successfully minimize the damage from electrical injury.

The use of P188 to seal permeabilized membrane was first described in 1992 [8]. Since that time, multiple investigators have independently described the capability of P188 to restore structural integrity of cell membranes [9–11]. In the past five years, physicochemical mechanisms that explain P188's ability to seal stable defects in membranes were well described [12,13]. It is now known that P188 preferably absorbs into disrupted membranes, changes the interfacial tension and then induces the membrane to seal [12,13]. Once the membrane is sealed the P188 is effectively squeezed out of the intact membrane [12]. The P188 is ideally suited for the task of sealing perforated cell membranes.

Over the past half-century, P188 has been routinely used in humans for various clinical purposes. It has been employed as a rheologic agent for blood banking and as an inhibitor of hemolysis in extra corporal membrane oxygenations. P188 is also commonly used today as a cofactor in various rheologic drugs that are weakly soluble in water. Unsuccessful attempts have been made to treat disease such as sickle cell anemia and myocardial infarction with the use of these surfactants as rheologic agents [32]. Thus, the pharmacokinetics of these agents in animals and humans are well established and their safety track record is well known [33, 34]. An intravenous injection of P188 is cleared in normal healthy human and animals with a half-life of 2–3 hours by excretion into the urine. Previous investigators using P188 as a rheologic agent have continuous infusions of this drug for several days [33,34]. Present results demonstrated that a single P188 bolus was sufficient for damaged cells that are accessible to the circulation to regain their structural integrity. The kinetics of membrane sealing following the exposure of P188 to damage cell membranes is almost instantaneous [13] relative to the after life of drug in serum. Therefore, intravenous injections with P188 can prove successful in sealing and restoring integrity of electroporatred cell membranes. The success of this mode of therapy is noteworthy because it can avoid some of the complications due to high dose continuous therapy [35,36]. In the high dose continuum therapy, some volunteers in clinical trials accused muscle pain in the legs and back [35]. Renal failure (azotemia) was also reported in 12% patients treated for acute myocardial infraction [36].

Acknowledgements

The authors wish to thank Dr. Hanne Gissel for guiding and assisting us the method for harvesting the leg muscles for the MRI experiments. The research presented here has been supported by NIH grants R01-GM61101(RCL), R01-GM64757-04 (RCL).

References

1. Bier M, Hammer SM, Canaday DJ, Lee RC. Kinetics of sealing for transient electropores in isolated mammalian skeletal muscle cells. Bioelectromagnetics 1999;20:194–201. [PubMed: 10194562]
2. Lee RC, Gaylor DC, Bhatt D, Israel DA. Role of cell membrane rupture in the pathogenesis of electrical trauma. J Surg Res 1988;44:709–719. [PubMed: 3379948]
3. Lee, RC.; Burke, JF.; Cravalho, EG., editors. Electrical Trauma: The Pathophysiology, Manifestations, and Clinical Management. Cambridge University Press; 1992.
4. Tropea BI, Lee RC. Thermal Injury Kinetics in Electrical Trauma. J Biomech Engr 1992;114:241–250.
5. Despa F, Orgill DP, Newalder J, Lee RC. The Relative Thermal Stability of Tissue Macromolecules and Cellular Structure in Burn Injury. Burns 2005;31:568–577. [PubMed: 15993302]
6. Block TA, Aarsvold JN, Matthews KL 2nd, Mintzer RA, River LP, Capelli-Schellpfeffer M, Wollman RL, Tripathi S, Chen CT, Lee RC. The 1995 Lindberg Award. Nonthermally mediated muscle injury and necrosis in electrical trauma. J Burn Care & Rehab 1995;16:581–588.
7. Miyake K, McNeil PL. Mechanical injury and repair of cells. Crit Care Med 2003;31:S496–S501. [PubMed: 12907878]
8. Lee RC, River LP, Pan FS, Wollmann RL. Surfactant-induced sealing of electropermeabilized skeletal muscle membranes in vivo. Proc Natl Acad Sci 1992;89:4524–4528. [PubMed: 1584787]
9. Marks JD, Pan CY, Bushell T, Cromie W, Lee RC. Amphiphilic, tri-block copolymers provide potent membrane-targeted neuroprotection. FASEB J 2001;15:1107–1109. [PubMed: 11292683]
10. Greenebaum B, Blossfield K, Hannig J, Carrillo CS, Beckett MA, Weichselbaum RR, Lee RC. Poloxamer 188 prevents acute necrosis of adult skeletal muscle cells following high-dose irradiation. Burns 2004;30:539–547. [PubMed: 15302418]
11. Serbest G, Horwitz J, Barbee K. The effect of poloxamer-188 on neuronal cell recovery from mechanical injury. J Neurotrauma 2005;22:119–132. [PubMed: 15665607]
12. Maskarinec SA, Hannig J, Lee RC, Lee KY. Direct observation of poloxamer 188 insertion into lipid monolayers. Biophys J 2002;82:1453–1459. [PubMed: 11867460]
13. Wu G, Majewski J, Ege C, Kjaer K, Weygand MJ, Lee KY. Interaction between lipid monolayers and poloxamer 188: an X-ray reflectivity and diffraction study. Biophys J 2005;2005;89:3159–3173. [PubMed: 16100276]
14. Firestone MA, Wolf AC, Seifert S. Small-angle X-ray scattering study of the interaction of poly (ethylene oxide)-b-poly(propylene oxide)-b-poly(ethylene oxide) triblock copolymers with lipid bilayers. Biomacromolecules 2003;4:1539–1549. [PubMed: 14606878]
15. Clausen, T. Na^+-K^+ pump stimulation improves contractility in damaged muscle fibers. In: Lee, RC.; Despa, F.; Hamann, KJ., editors. Cell Injury: Mechanisms, Responses, and Repair. 1066. Ann NY Acad. Sci; New York: 2005. p. 286-294.
16. Haacke, EM.; Brown, RW.; Thompson, MR.; Venkatesan, R. Magnetic Resonance Imaging: Physical Principles and Sequence Design. 1. New York: John Wiley and Sons; 2005.
17. Barratt TM, Walser M. Extracellular fluid in individual tissues and in whole animals: the distribution of radiosulfate and radiobromide. J Clin Invest 1969;48:56–66. [PubMed: 5765027]
18. Gissel, H.; Despa, F.; Collins, J.; Mustafi, D.; Rojan, K.; Karczmar, G.; Lee, RC. Magnetic Resonance Imaging of Changes in Muscle Tissue Following Membrane Trauma. In: Lee, RC.; Despa, F.; Hamann, KJ., editors. Cell Injury: Mechanisms, Responses, and Repair. 1066. Ann NY Acad Sci; New York: 2005. p. 272-285.
19. Rasband, WS.; Image, J. U. S. National Institutes of Health; Bethesda, Maryland, USA, : 1997–2005. http://rsb.info.nih.gov/ij/
20. Abramov GS, Bier M, Capelli-Schellpfeffer M, Lee RC. Alteration in sensory nerve function following electrical shock. Burns 1996;22:602–606. [PubMed: 8982537]

21. Merletti R, Lo Conte L, Avignone E, Guglielminotti P. Modeling of surface myoelectric signals – Part I: Model implementation. IEEE Trans Bio-Med Eng 1999;46:810–820.
22. Ababneh Z, Beloeil H, Berde CB, Gambarota G, Maier SE, Mulkern RV. Biexponential parametrization of T2 and diffusion decay curves in a rat muscle edema model: Decay curve components and water compartments. Magn Reson Med 2005;54:524–531. [PubMed: 16086363]
23. Foley JM, Jayaraman RC, Prior BM, Pivarnik JM, Meyer RA. MR measurements of muscle damage and adaptation after eccentric exercise. J Appl Physiol 1999;87:2311–2318. [PubMed: 10601183]
24. Saab G, Thompson RT, Marsh GD. Multicomponent T2 relaxation of in vivo skeletal muscle. Magn Reson Med 1999;42:150–157. [PubMed: 10398961]
25. Gamborata G, Cairns BE, Berde CB, Mulkern RV. Osmotic effects on the T2 relaxation decay of In vivo muscle. Magn Reson Med 2001;46:592–599. [PubMed: 11550254]
26. Bertram HC, Karlsson AH, Rasmussen M, Pedersen OD, Donstrup S, Andersen HJ. Origin of multiexponential T(2) relaxation in muscle myowater. J Agric Food Chem 2001;49:3092–3100. [PubMed: 11410014]
27. Matthews KL, Aarsvold JN, Mintzer RA, Chen C-T, Lee RC. Tc-99m pyrophosphate imaging of poloxamer-treated electroporated skeletal muscle in an in vivo rat model. Burns. 2006In press
28. Fleckenstein, JL. Skeletal muscle evaluated by MRI. In: Grant, DM.; Harris, RK., editors. Encyclopedia of Nuclear magnetic Resonance. Chister; UK: 1996. p. 4430-4436.
29. Serbest G, Horwitz J, Barbee K. The effect of poloxamer-188 on neuronal cell recovery from mechanical injury. J Neurotrauma 2005;22:119–132. [PubMed: 15665607]
30. Yasuda S, Townsend D, Michele DE, Favre EG, Day SM, Metzger JM. Dystrophic heart failure blocked by membrane sealant poloxamer. Nature 2005;436:1025–1029. [PubMed: 16025101]
31. Baskaran H, Toner M, Yarmush ML, Berthiaume F. Poloxamer-188 improves capillary blood flow and tissue viability in a cutaneous burn wound. J Surg Res 2001;101:56–61. [PubMed: 11676555]
32. Orringer EP, Casella JF, Ataga KI, Koshy M, Adams-Graves P, Luchtman-Jones L, Wun T, Watanabe M, Shafer F, Kutlar A, Abboud M, Steinberg M, Adler B, Swerdlow P, Terregino C, Saccente S, Files B, Ballas S, Brown R, Wojtowicz-Praga S, Grindel JM. Purified Poloxamer 188 for Treatment of Acute Vaso-occlusive crisis of Sickle Cell Disease: A Randomized Controlled Trial. JAMA 2001;286:2099–2106. [PubMed: 11694150]
33. Grindel JM, Jaworski T, Piraner O, Emanuele RM, Balasubramanian M. Distribution, Metabolism, and Excretion of a Novel Surface-Active Agent, Purified Poloxamer 188, in Rats, Dogs, and Humans. J Pharma Scie 2002;91:1936–1947.
34. Grindel JM, Jaworski T, Emanuele RM, Culbreth P. Pharmacokinetics of a Novel Surface-Active Agent, Purified Poloxamer 188, in Rat, Rabbit, Dog and Man, Biopharm. Drug Dispos 2002;23:87–103.
35. Jewell RC, Khor SP, Kisor DF, LaCroix KAK, Wargin WA. Pharmacokinetics of RheothRx injection in healthy male volunteers. J Pharm Scie 1997;86:808–812.
36. O'Keefe JH Jr, Grines CL, DeWood MA, Schaer GL, Browne K, Magorien RD, Kalbfleisch JM, Fletcher WO Jr, Bateman TM, Gibbons RJ. Poloxamer-188 as an Adjunct to Primary Percutaneous Transluminal Coronary Angioplasty for Acute Myocardial Infarction. Am J Cardiol 1996;78:747–750. [PubMed: 8857476]

List of abbreviations

ATP
adenosine triphosphate

BFM
biceps femoris muscles

CMAP
compound muscle action potential

CMC
critical micelle concentration

CPMG
Carr-Purcell-Meiboom-Gill

EDL
extensor digitorum longus

EMG
electromyography

H&E
hematoxylin and eosin

IP
intraperitoneal

IV
intravenous

KCl
potassium chloride

LR
lactated Ringers

MR
magnetic resonance

MRI
magnetic resonance imaging

P188
poloxamer 188

SaO2%
blood oxygen saturation

SOL
soleus

ST
slice thickness

T1
spin-lattice relaxation time

T2
spin-spin relaxation time

TR
repetition time

TE
echo time

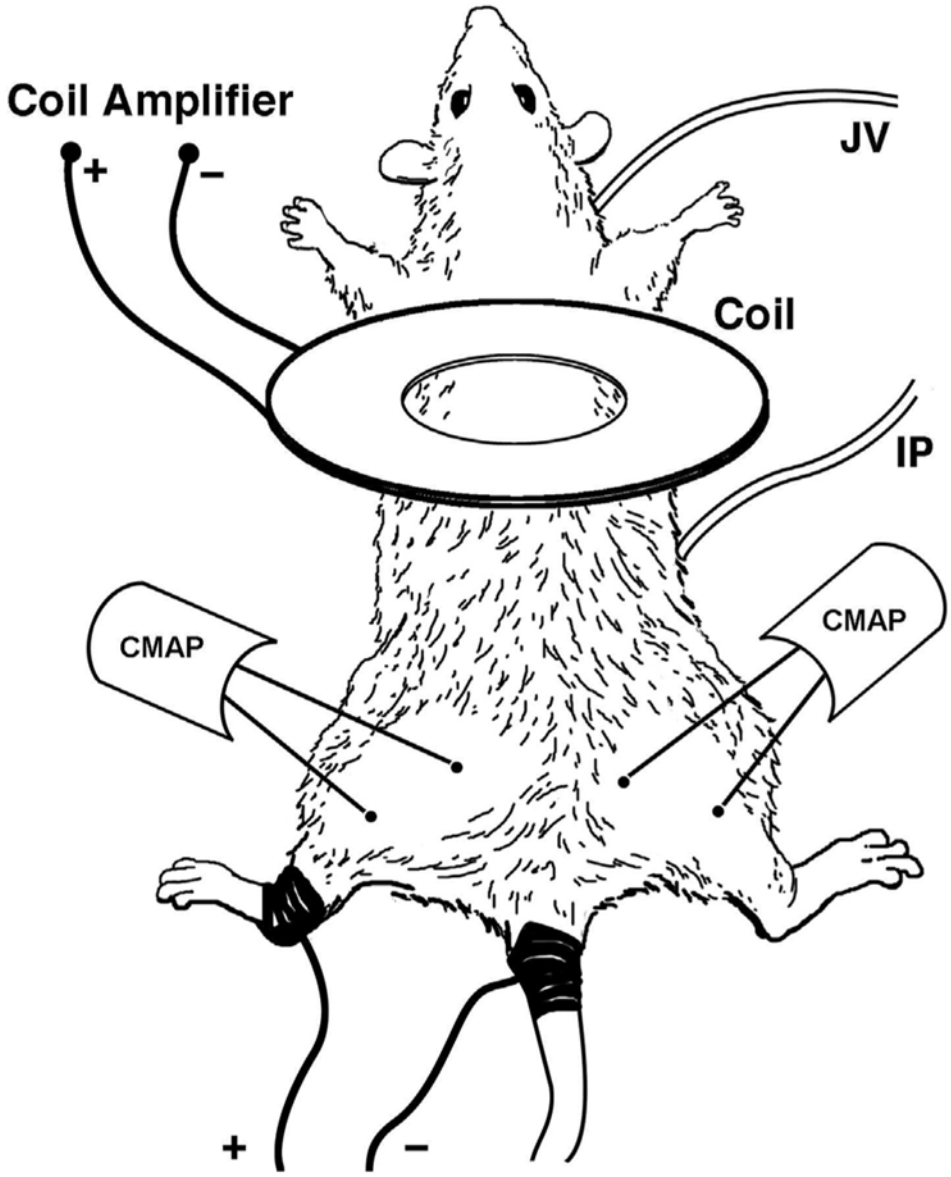

Figure 1.
Illustration depicting anesthetic and treatment injection sites (IP, JV respectively), hind limb electroporation path (dark areas of tail and left leg), and CMAP stimulation (Coil) and recording sites (CMAP) on anesthetized rat.

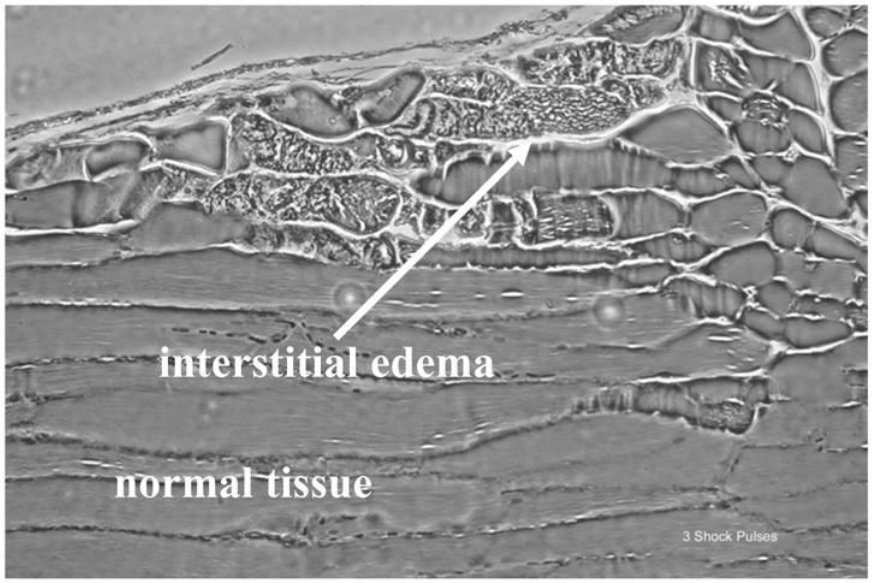

(a)

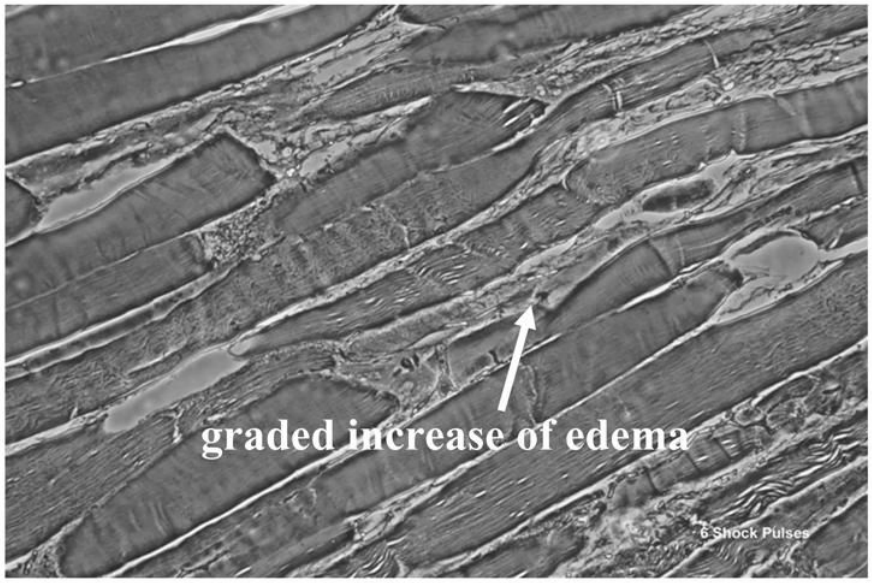

(b)

(c)

Figure 2.

Representative phase contrast photomicrographs (40x) of H&E stained 7 μm sections of electrically shock biceps femoris muscles are shown. Electroporation damage is distributed very non-uniformly in each muscle reflecting the stochastic nature of electroporation. The more shocks the more severe and the more uniform the damage. Longitudinal sections from muscle exposed to (a) 3 shock pulses exhibit a low percentage of damaged cells with mostly normal cytoskeletal architecture and some interstitial edema; (b) muscles subjected to 6 shocks manifest damage to 20–30% of the cells with more edema and (c) muscle subjected to 12 shocks have marked "contraction-band necrosis" to most cells and severe edema. Biopsies were taken 6 hours after electrical shock.

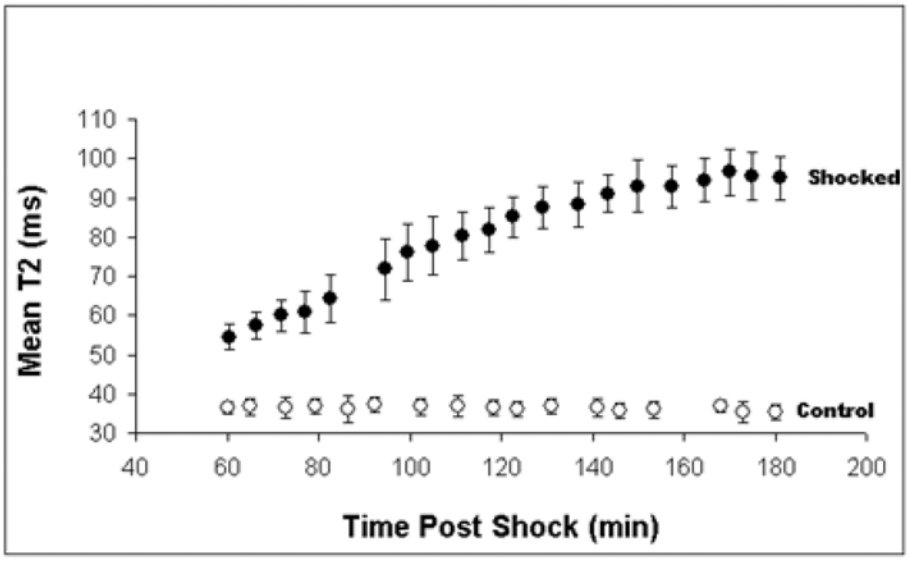

Figure 3.

Plot characterizing the development of edema injury over time. A 5 x 5 mm ROI was selected, and mean T_2 values in a shocked leg (closed circles, ± SD, n = 25 pixels) and non-shocked leg (open circles, ± SD, n = 25 pixels) as a function of time after electroporation. In this case lactated ringers was used as treatment and injured tissue was followed over time

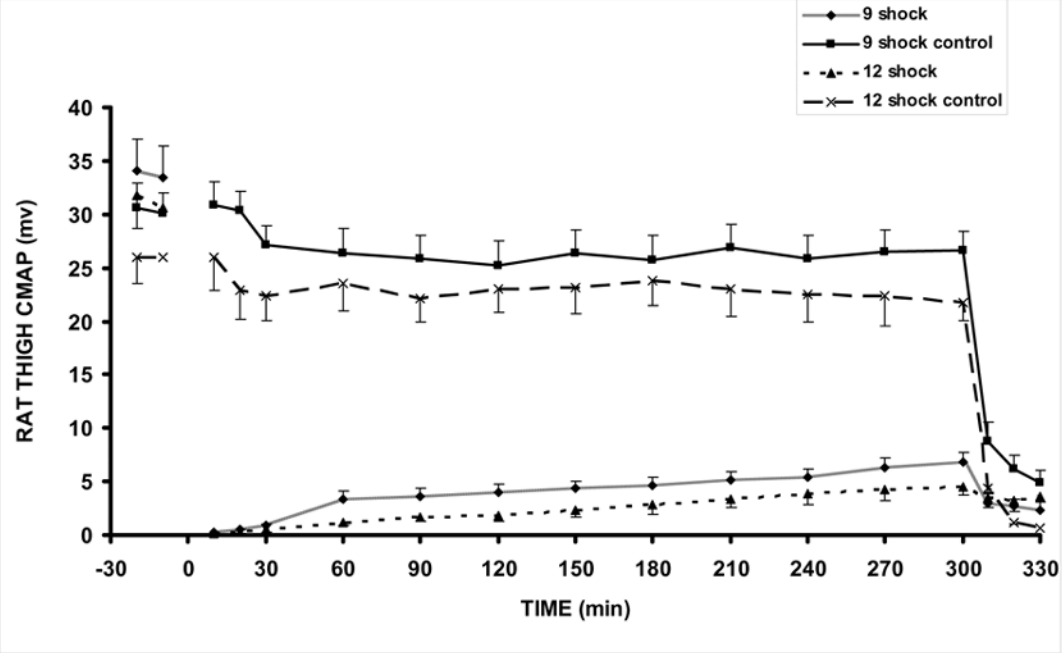

Figure 4.

CMAP amplitudes in control and injured legs of rats receiving 9 and 12 shocks, respectively 12 shock (n=10), 12 shock control (n=8), 9 shock (n=17), 9 shock control (n=15). All animals received control LR treatment. At 5h, the sciatic nerve is blocked with lidocaine to verify that CMAP is nerve stimulated.

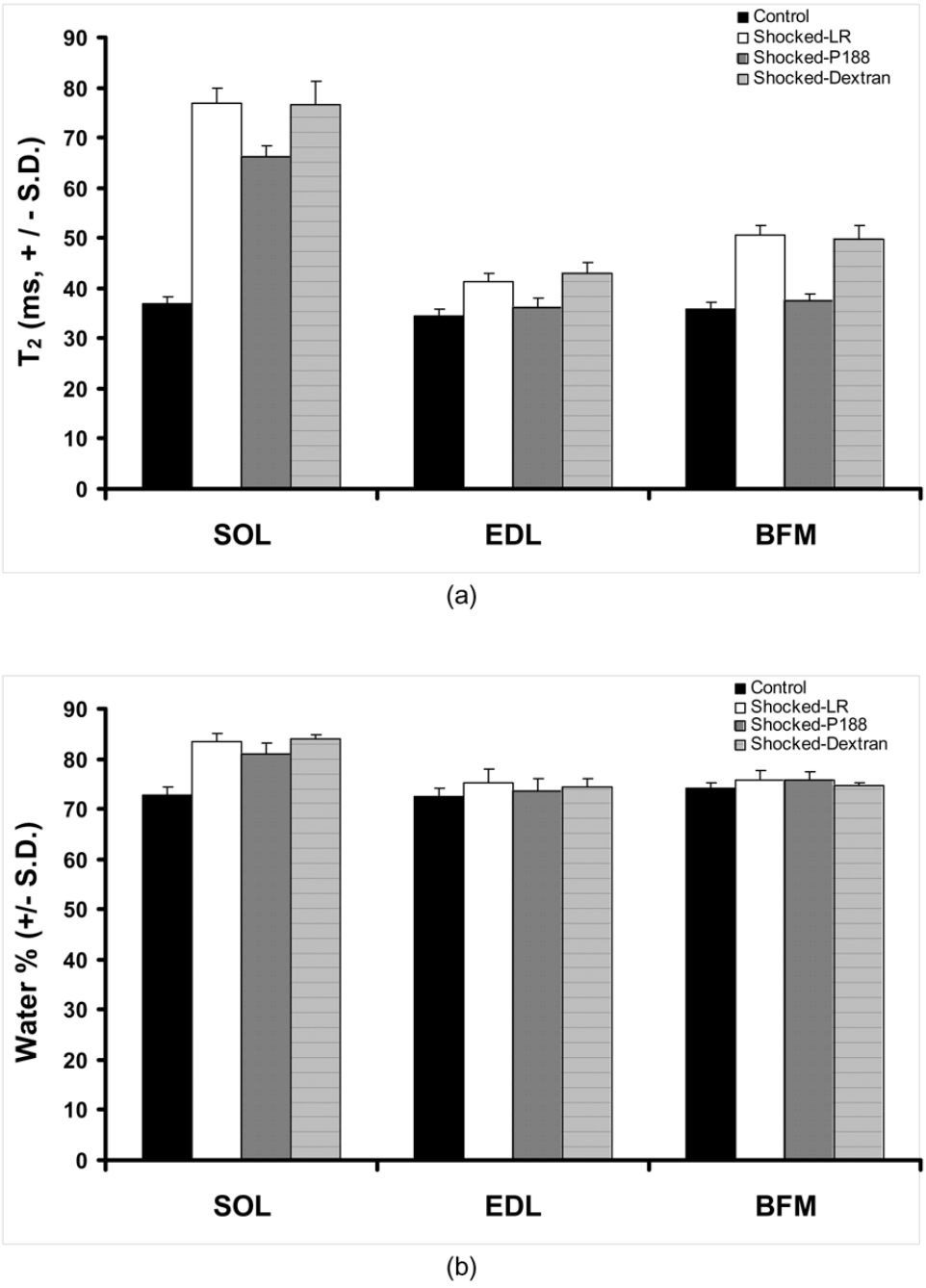

Figure 5.

(a) Plot of T_2 values for three different muscle samples. (b) The characteristic hydration levels for muscle samples of interest. SOL – soleus, EDL – extensor digitorum longus, BFM – biceps femoris muscle. All animals received a 1 mL bolus treatment as described. For each treatment of all muscles, n = 5. Two sets of p-values were calculated to determine treatment significance. P188, between shocked LR and P188-treated muscle samples; Dextran, between shocked LR and Dextran-treated muscle samples. The first set is: p = 0.046 (SOL), p = 0.042 (EDL) and p = 0.952 (BFM). The second set of p- values is: p = 0.728 (SOL), p = 0788 (EDL) and p = 0.578 (BFM)

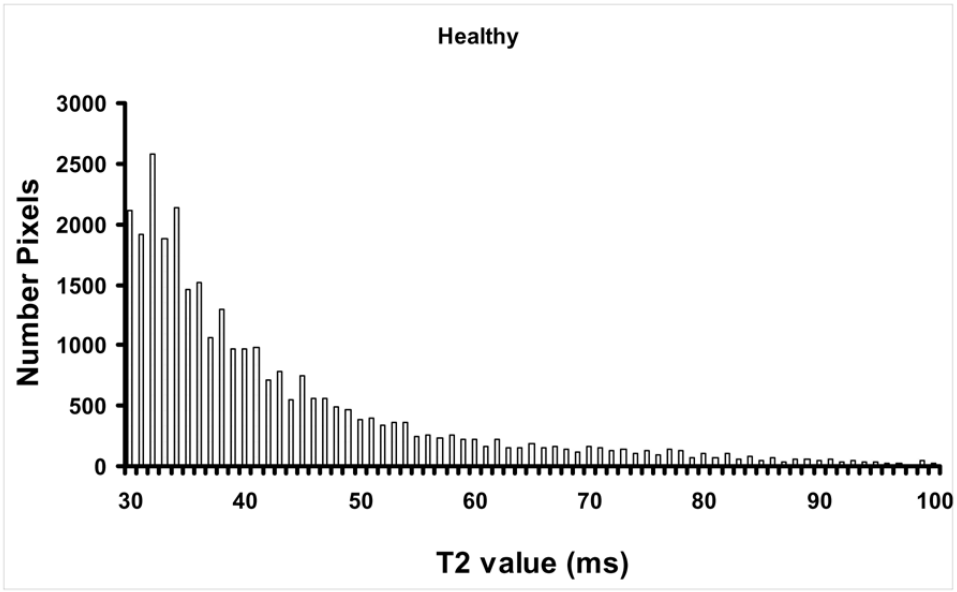

(a)

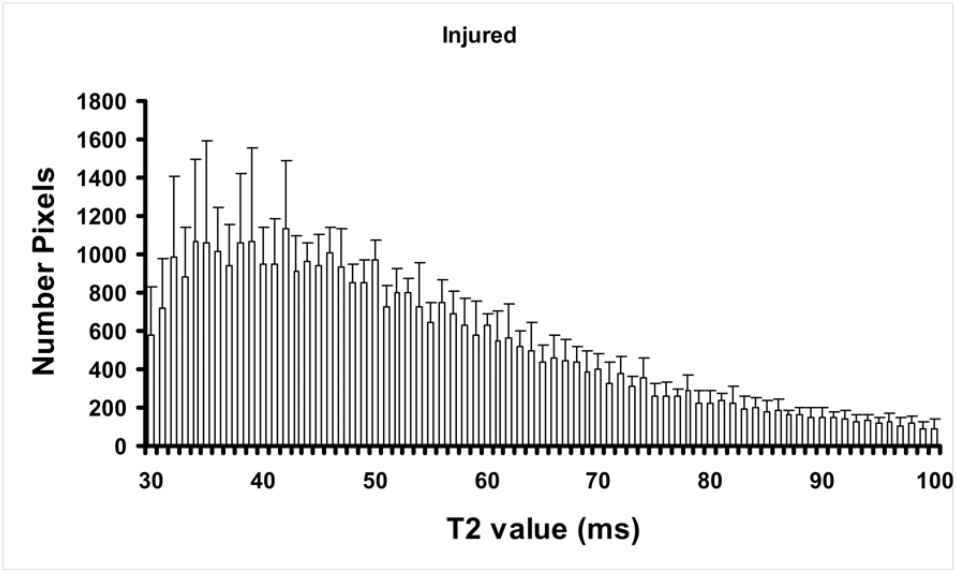

(b)

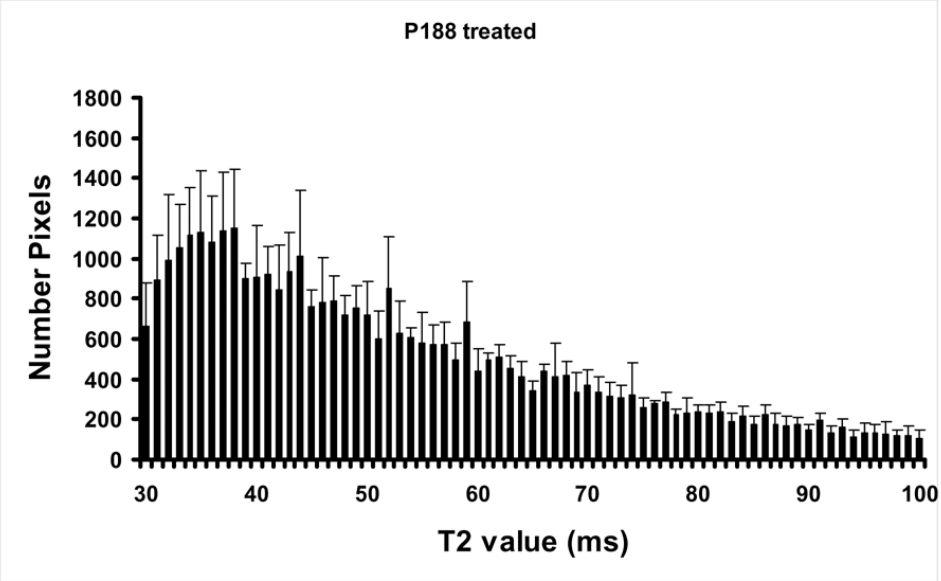

(c)

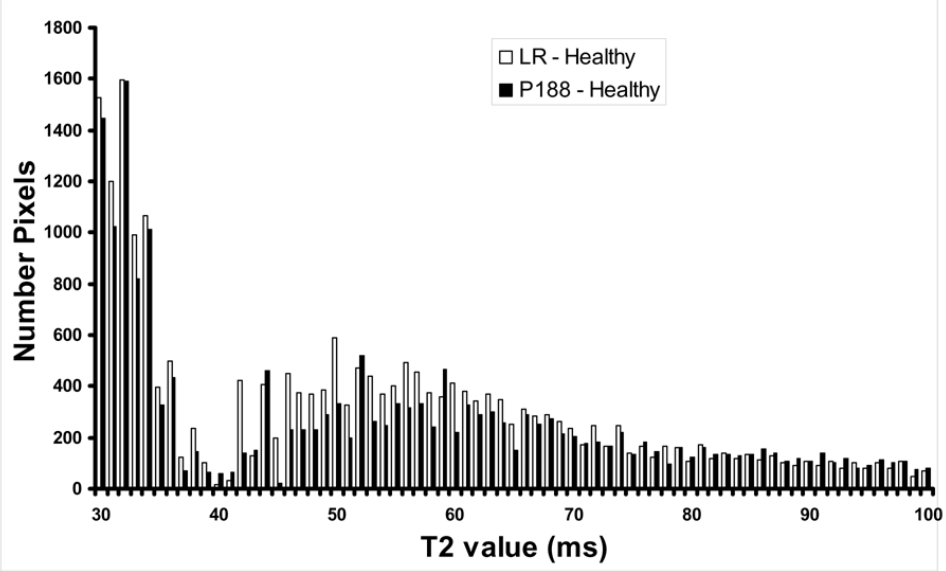

(d)

Figure 6.

Average number of pixels for each T_2 value in the interval 30–100 ms for healthy (a) LR-treated (b) and P188-treated (c) rats; In (d), we can see the difference in the magnetic signal intensity distribution between P188-treated and healthy rats (bright) and between LR-treated rats and healthy rats (dark) suggesting the evolution of the volume of injury (n = 5).

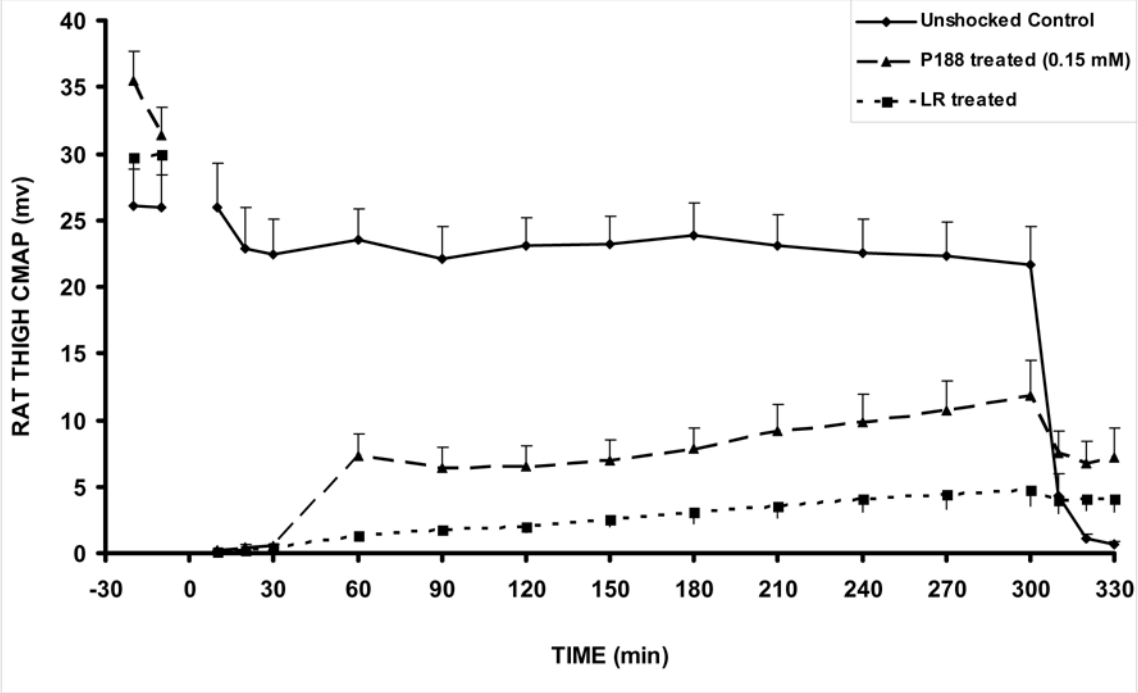

Figure 7.

CMAP amplitudes in control, shocked (LR-treated), and shocked P188-treated rats. At 5h, the sciatic nerve is blocked with lidocaine to verify that CMAP is nerve stimulated. The unshocked contralateral control leg CMAP values were not significantly different between LR-treated and P188-treated groups, so control data was obtained from the LR-treated group as shown. Unshocked Control (n=8), P188 treated (n=3), LR treated (n=8). All animals received 9 shocks. All values are shown as mean +/− SEM. p = 0.0270. This is the two tailed p value calculated from an unpaired t-test at the 300 minute time point, comparing shocked P188 treated to shocked LR treated.

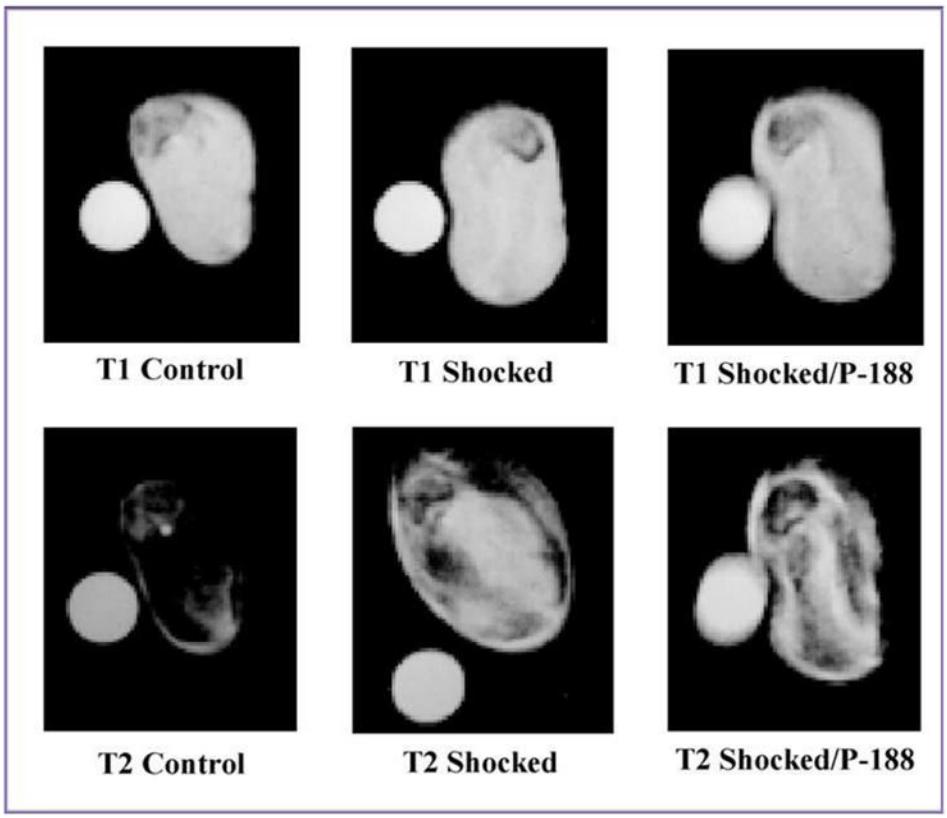

Figure 8.

The greyscale contrast for characteristic T_1 and T_2 - weighted MRI images of control (left), injured (middle) and P188 treated (right) muscle samples suggesting the recovery of the water balance across the plasma membrane after the treatment with P188. One can observe that the grey level characterizing the magnetic signal of water in P188 treated muscle samples is approaching that corresponding to the control muscle samples. The parameters for recording T_1 - weighted MRI images were TR = 400 ms and TE = 5 ms. T_2 - weighted MRI images correspond to TR = 2s and TE = 60 ms.